Marshall Plan Scholarship Report

System Layer Modeling in Cellular Mobile Communication Systems

Martin Taranetz
martin.taranetz@nt.tuwien.ac.at

April 2014

Advisors

Prof. Markus Rupp
Vienna University of Technology

Prof. Robert W. Heath Jr.
The University of Texas at Austin

Contents

Preface

This report outlines my investigations as a visiting scholar at the University of Texas at Austin. It comprises a peer reviewed conference paper and extended work.

First and foremost I want to thank my advisor Prof. Dr. Markus Rupp, whose good contacts to Prof. Robert W. Heath Jr. made this work possible. Being surrounded by world-renowned experts offered an amazing working environment and greatly enhanced scientific work towards my PhD.I also want to thank Mrs. Angelika Schweighart for her commitment and guidance through the scholarship application.

Finally, I want to express my deep gratitude for the support of the Austrian Marshall Plan Foundation, which helped me to overcome the financial burden and enabled an experience which by far exceeded academic life.

"What starts here changes the world."
(Walter Cronkite)

Abstract

This paper presents a system model that enables the analysis of *indoor* downlink performance in urban two-tier heterogeneous cellular networks. The urban building topology is modeled as a process of randomly distributed circles. Each building is deployed with an indoor small cell with a certain *occupation probability*. Macro base stations are sited outdoors. Their signals experience *distance-dependent shadowing* due to the blockage of the buildings. Given a typical building at the origin, expressions for the coverage probability with- and without small cell occupation are derived. The analysis of the asymmetric interference field as observed by a typical indoor user is simplified by approximations. Their accuracy is verified by Monte Carlo simulations. Our results show that isolation by wall partitioning can enhance indoor rate, and that the improvement is more sensitive to building density, rather than penetration loss per building.

1 Introduction

There is a broad consensus among communication engineers that two of the key characteristics of future wireless cellular networks are *spatial randomness* and *heterogeneity* [1–14]. Yet, numerous studies have met the challenge of finding representative, analytically tractable models for the emerging systems, most of which are based on techniques from stochastic geometry [7, 11, 15]. However, when it comes to convenient expressions, this mathematical framework imposes its own particular limitations [1, 14]. Firstly, in the analysis on stochastic geometry, *shadowing* is typically incorporated by log-normally distributed Random Variates (RVs) [8, 12, 13] or neglected at all [1–7, 9, 10]. A recent study on blockage effects in urban environments indicates a dependency on the link length [16]. It follows the intuition that a longer link increases the likelihood of buildings to intersect with it. Secondly, scenarios comprising *both indoor- and outdoor environments* have not received much attention in analytical studies due to the imposed inhomogeneities on signal propagation. The designated area of operation for small cells is indoors. Existing approaches either neglect the wall partitioning [8, 17], oversimplify the macro-tier topology [4–6] or the omit cross-tier interference [12]. Considering a two-tier cellular network with outdoor macro Base Stations (BSs) and indoor-deployed small cells, our contributions are:

- A tractable model for urban environment topologies. It comprises an outdoor environment, which is partly covered by circular building objects with a certain density. Based on concepts from random shape theory, the model is applied to characterize both *signal propagation* and *network deployment*.
- A novel *virtual building approximation* to simplify aggregate-interference analysis. The key idea is to establish a user-centric interference environment

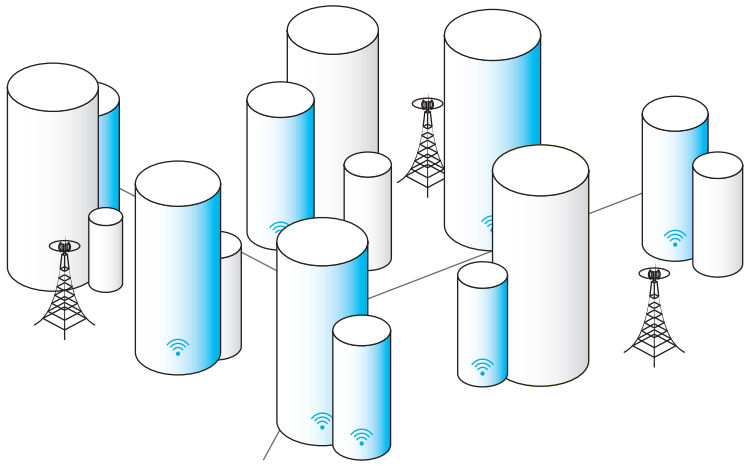

Figure 1: Two-tier cellular network deployment in dense urban environment. Macro BS are sited outdoors. Buildings are deployed with indoor small cells with a certain occupation probability.

by shifting the centers of the typical building and its exclusion regions to the user location.

- Analytical expressions for the *coverage probability* of indoor users with small cell- and macro BS association, assuming that a building is served by a small cell with a certain *occupation probability*.
- Evaluation of the spectral efficiency of *typical* indoor users with respect to building density, wall penetration loss and small cell occupation probability.

2 System Model

2.1 Topology Model for Urban Environments

Consider a two-tier cellular network comprising outdoor BSs and indoor small cells, as shown in Figure 2. Buildings are modeled by a Boolean scheme of circles on the $\mathbb{R}^2$ plane. Therefore, the centers of the circles form a Poisson Point Process (PPP) Φ_{B} of intensity λ_{B} [18]. For simplicity, we assume that all circles have a fixed radius R_{I}. A point on the plane is said to be *indoors*, if it is covered by a building, and *outdoors* otherwise. Indoor- and outdoor environment are partitioned by wall penetration loss, which is hereafter denoted as L_W and assumed constant for all buildings.

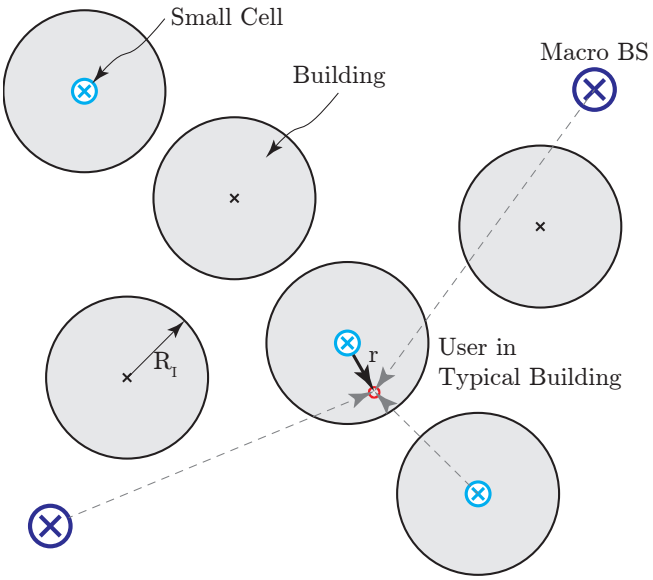

Figure 2: Urban two-tier heterogeneous cellular network. Macro BSs are deployed in an outdoor environment. Buildings are modelled as a random process of circles and are assumed to have a fixed radius R_{I}. Only a fraction of buildings is occupied by small cells. The figure depicts a typical indoor user with macro BSs and neighboring small cells (dashed lines).

2.2 Network Deployment

Macro BSs are distributed according to a PPP Φ_{M} of intensity μ_{M}. Note that we require these BSs to be located outdoors. Thus, the macro BS process can equivalently be constructed by independently thinning an initial PPP of density $\mu'_{\mathrm{M}} = \mu_{\mathrm{M}}/p_{\mathrm{O}}$, where p_{O} equals the probability that a point on $\mathbb{R}^2$ is not covered by a building. According to [16, Corollary 1.2], the thinning probability is $p_{\mathrm{O}} = \exp(-\lambda_{\mathrm{B}} R_{\mathrm{I}}^2 \pi)$.
A building will deploy an indoor small cell with a certain *occupation probability* η. Assume the indoor small cells to be located at the center points of the occupied buildings. Then, their spatial distribution can be modeled by a PPP Φ_{S} of intensity $\lambda_{\mathrm{B}}\,\eta$, which results from independently thinning the object center PPP Φ_{B} [18].

2.3 User Association

In this paper, we aim to characterize the coverage and rate performance of indoor users. Noting that the buildings are assumed to form a Boolean scheme, the centers of the buildings form a PPP on the plane [16]. Therefore, by Slivnyak's theorem [18], when fixing a typical building at the origin, the centers of the other buildings still form a PPP. We will investigate the performance of users inside

the typical building. We define separate association rules, depending on whether or not the typical building is occupied by a small cell.

Case 1 *[Typical Building with Small Cell]:* Consider a typical building at the origin, which is equipped with an indoor small cell. For simplicity, we assume that all users inside this building are associated with the small cell at the origin. We omit the cases in which indoor users at the edge of the typical building may receive stronger signals from a close-by outdoor macro BS, thus underestimating the coverage probability. Similar to the analysis in [11], *exclusion guard regions* are imposed on both macro- and small cell tier, where no BSs from the corresponding tier are allowed to distribute. For simplicity, we assume that the exclusion region for macro BSs is a ball of radius R_{I} centered at the origin, ensuring that no macro BSs are located inside the typical building. The exclusion region of the small cell tier is defined as a ball of radius $2\,R_{\mathrm{I}}$ in order to prevent overlapping association regions of two small cells.

Case 2 *[Typical Building without Small Cell]:* When the typical building is not occupied by a small cell, the user is either associated to the dominant macro BS or a small cell in the immediate vicinity. We regard the former as being of greater relevance and omit the latter, which leads to a lower bound on coverage probability. In this case, the indoor user will be served by the nearest BS of the macro tier. The same exclusion regions as defined in Case 1 are employed for macro BSs and small cells.

2.4 Virtual Building Approximation

Without loss of generality, a *typical indoor user* is assumed to be located at $(r, 0)$. Note that the exclusion regions as defined in Section 2.3 are centered at the origin rather than at the user. Consequently, the interference field as observed by the user is asymmetric and renders analysis difficult in general. Thus, we propose the following approximation.

Let (R, θ) denote the position of an interference. Its distance to a user located at $(r, 0)$ is determined as

$$d(r) = \sqrt{R^2 + r^2 - 2Rr\cos\theta}. \tag{1}$$

Since typically $R \gg r$, we approximate $d(r)$ as

$$d(r) \approx R, \tag{2}$$

which is independent of the angle θ. As shown in Figure 3, the approximation in (2) is equivalent to shifting all the BSs along with the exclusion regions by a vector $(r, 0)$, as if the typical building was centered at the user location. Thus, this approach is referred to as *virtual building approximation*, and is applied to simplify further analysis.

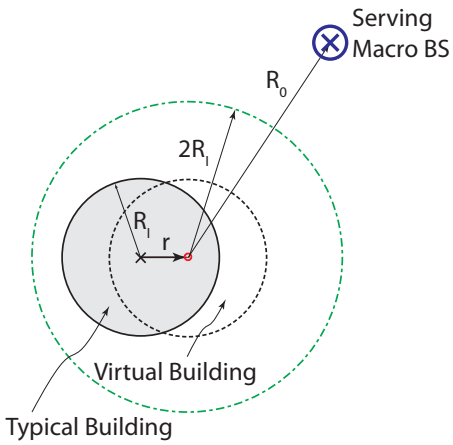

Figure 3: Target area without small cell (gray shaded) and user-centric *virtual building* (dashed). Dashed-dotted circles denotes the shifted small cell exclusion region. The indoor user is assumed to be served by the nearest Macro BS at distance R_0.

2.5 Signal Propagation

2.5.1 Macro BS to Indoor User

A signal originating from a macro BS experiences small scale fading, log-distance dependent path loss with path loss exponent α_{O}, attenuation due to building blockage and wall penetration, L_{W}. Small scale fading is modeled by a Rayleigh RV g_i, with $\mathbb{E}[g_i] = 1$. Along the lines of [16, Theorem 1], the number of obstructing blockages along a link of length R is a Poisson RV with parameter $\beta_{\mathrm{B}} R$, where $\beta_{\mathrm{B}} = 2\lambda_{\mathrm{B}} R_{\mathrm{I}}$ in the introduced topology model. For analytical tractability we employ the *expected blockage attenuation*, as referred from [16, Theorem 6]. Combining blockage- and log-distance path loss along a link of length R yields

$$\ell(R) = e^{-\beta_{\mathrm{B}} R(1-\gamma_{\mathrm{B}})} R^{-\alpha_O}, \tag{3}$$

where γ_{B} refers to the attenuation of a single blockage, also denoted as *building penetration loss*. Note that (3) characterizes *shadowing* entirely by the parameters of the underlying environment topology and accounts for the condition that the macro BS is deployed outdoors.

2.5.2 Small Cell to Indoor User

When user and small cell are situated in the same building, the signal experiences small scale fading and log-distance path loss with exponent α_{I}.
The signals from all other small cells are subject to small scale fading, log-distance

path loss with exponent α_{O} and attenuation by a factor L_{W}^2, as caused by the indoor-to-outdoor and outdoor-to-indoor wall penetration. Since small cell transmit power is typically low, only small cell interferers from *neighboring* buildings are taken into account. We define two building as being *neighbors* to each other, if the segment connecting their centers is not intersected by any other building.

3 Performance Analysis

In this section we derive analytical expressions for the coverage probability of an indoor users at position $(r, 0)$, regarding both buildings with- and without small cell deployment. We assume the network to be interference limited, as is typically the case in urban areas [19]. Thus, thermal noise is neglected in the analysis.

3.1 Typical Building with Small Cell

Assume the typical building to be occupied by a small cell. Then, the Signal-to-interference-ratio (SIR) at distance r, $0 < r \leq R_{\mathrm{I}}$, is determined as

$$\mathrm{SIR}^{(\mathrm{S})}(r) = (P_{\mathrm{S}} g_0 r^{-\alpha_{\mathrm{I}}}) \left(\sum_{i:R_i > R_{\mathrm{I}}} P_{\mathrm{M}} g_i L_{\mathrm{W}} \ell(R_i) + \sum_{i:R_i > 2R_{\mathrm{I}}} S_i P_{\mathrm{S}} g_i L_{\mathrm{W}}^2 R_i^{-\alpha_{\mathrm{O}}} \right)^{-1}, \tag{4}$$

where the terms P_{M} and P_{S} denote macro BS- and small cell transmit powers, $\ell(\cdot)$ corresponds to the combined blockage- and path loss attenuation, as defined in (3) and R_i refers to the length of link i. The RVs S_i are Bernoulli distributed and, by [16, Theorem 1], have parameters $\exp(-\beta_{\mathrm{B}} R_i - p_{\mathrm{B}})$, where $p_{\mathrm{B}} = \lambda_{\mathrm{B}} R_{\mathrm{I}}^2 \pi$. They indicate whether or not an interfering small cell is in a neighboring building of the typical user.

Theorem 1 *Consider a user at distance r, $0 < r \leq R_{\mathrm{I}}$, away from the center of a small cell-occupied building. Then, its coverage probability is determined as*

$$P_c^{(\mathrm{S})}(\delta | r) = \mathbb{P}\left[\mathrm{SIR}^{(\mathrm{S})}(r) > \delta | r\right] = e^{-2\pi(\mu_{\mathrm{M}} I_{\mathrm{M}} + \mu_{\mathrm{S}} I_{\mathrm{S}})}, \tag{5}$$

where

$$I_{\mathrm{M}} = \int_{R_{\mathrm{I}}}^{\infty} \left(1 - \frac{\frac{P_{\mathrm{S}}}{P_{\mathrm{M}}}}{\frac{P_{\mathrm{S}}}{P_{\mathrm{M}}} + \delta\, \ell(t) L_{\mathrm{W}} r^{\alpha_{\mathrm{I}}}} \right) t\, dt \tag{6}$$

$$I_{\mathrm{S}} = \int_{2R_{\mathrm{I}}}^{\infty} \left(\frac{\delta\, L_{\mathrm{W}}^2\, r^{\alpha_{\mathrm{I}}} e^{-(\beta_{\mathrm{B}} t + p_{\mathrm{B}})}}{t^{\alpha_{\mathrm{O}}} + \delta\, L_{\mathrm{W}}^2\, r^{\alpha_{\mathrm{I}}}} \right) t\, dt \tag{7}$$

Proof 1 *Applying (4), we exploit that g_i are i.i.d. exponential RVs and S_i are Bernoulli RVs with parameters* $\exp(-\beta_{\mathrm{B}} R_i - p_{\mathrm{B}})$. *Then, it follows from Campbell's theorem that*

$$\begin{aligned} P_c^{(\mathrm{S})}(\delta|r) &= \mathbb{P}\left[\mathrm{SIR}^{(\mathrm{S})}(r) > \delta | r\right] \\ &= \mathbb{E}_{\Phi_{\mathrm{M}}}\left[\prod_{i:R_i>R_{\mathrm{I}}} \frac{\frac{P_{\mathrm{S}}}{P_{\mathrm{M}}}}{\frac{P_{\mathrm{S}}}{P_{\mathrm{M}}} + \delta\, \ell(R_i) L_{\mathrm{W}} r^{\alpha_{\mathrm{I}}}}\right] \\ &\quad \mathbb{E}_{\Phi_{\mathrm{S}}}\left[\prod_{i:R_i>R_{\mathrm{S}}} \left(1 - \frac{\delta\, L_{\mathrm{W}}^2\, r^{\alpha_{\mathrm{I}}} e^{-(\beta_{\mathrm{B}} R_i + p_{\mathrm{B}})}}{R_i^{\alpha_{\mathrm{O}}} + \delta\, L_{\mathrm{W}}^2\, r^{\alpha_{\mathrm{I}}}}\right)\right] \end{aligned} \tag{8}$$

Finally, (5) is obtained by computing the Laplace functional [18].

3.2 Typical Building without Small Cell

Assume a dominant macro BS to be located at distance R_0, $R_0 > R_{\mathrm{I}}$ away from the center of the typical building and consider that this building is not occupied by a small cell. Then, the SIR at distance r, $0 < r \leq R_{\mathrm{I}}$, calculates as

$$\begin{aligned} &\mathrm{SIR}^{(\mathrm{M})}(R_0) \approx (M_{\mathrm{M}} g_0 \ell(R_0)) \\ &\left(\sum_{i:R_i>R_0} M_{\mathrm{M}} g_i \ell(R_i) + \sum_{i:R_{\mathrm{I}}>2R_{\mathrm{I}}} S_i M_{\mathrm{S}} g_i L_{\mathrm{W}} R_i^{-\alpha_{\mathrm{O}}}\right)^{-1} \end{aligned} \tag{9}$$

Note that (i) the expression is independent of r and (ii) the factor L_{W} is omitted, since attenuation due to wall penetration is experienced by all signals and therefore cancels out in the SIR term.

Theorem 2 *Consider a user at distance r, $0 < r \leq R_{\mathrm{I}}$, away from the center of a typical building without small cell and assume that it is associated with its dominant macro BS. Then, its coverage probability is determined as*

$$\begin{aligned} P_c^{(\mathrm{M})}(\delta) &= \mathbb{P}\left[\mathbb{E}_{R_0}\left[\mathrm{SIR}^{(M)}(R_0) > \delta\right]\right] \\ &= \int_{R_{\mathrm{I}}}^{\infty} P_c^{(\mathrm{M})}(\delta|R) f_{R_0}(R) dR, \end{aligned} \tag{10}$$

where

$$P_{\mathrm{c}}^{(M)}(\delta|R_0) = e^{-2\pi(\mu_{\mathrm{M}} I_{\mathrm{M}} + \mu_{\mathrm{S}} I_{\mathrm{S}})}, \tag{11}$$

Table 1: Simulation Parameters

Macro-to-small cell power ratio	$\frac{P_S}{P_M}$	10^{-2}
Macro BS density	μ_M	4.61×10^{-6} m^{-2}
Outdoor path loss exponent	α_O	4
Indoor path loss exponent	α_I	2
Radius of Building Area	R_I	25 m

with

$$I_M = \int_{R_0}^{\infty} \left(1 - \frac{\ell(R_0)}{\ell(R_0) + \delta\,\ell(t)}\right) t\,dt, \tag{12}$$

$$I_S = \int_{2R_I}^{\infty} \left(\frac{\delta L_W \frac{P_S}{P_M} e^{-(\beta_B t + p_B)}}{t^{\alpha_O}\ell(R_0) + \delta L_W \frac{P_S}{P_M}}\right) t\,dt, \tag{13}$$

and

$$f_{R_0}(R) = \begin{cases} 2\pi\mu_M R\, e^{-\pi\mu_M(R^2 - R_I^2)} & ,\ R \geq R_I \\ 0 & ,\ \text{otherwise} \end{cases}. \tag{14}$$

Proof 2 *The conditional coverage probability $P_c^{(M)}(\delta|R)$ in (31) is derived along the lines of (5). Deconditioning on the dominant macro BS distance leads to (30), where $f_{R_O}(R)$ in (34) is the nearest neighbor distance distribution of a homogeneous PPP outside a ball of radius R_I [20].*

3.3 Typical Indoor User

The coverage probability of a *typical* indoor user at distance r, $0 < r \leq R_I$, is obtained by linearly combining $P_c^{(S)}(\delta|r)$ from (5) and $P_c^{(M)}(\delta)$ from (30) according to the small cell occupation probability η. Then,

$$P_c(\delta|r) = \eta\, P_c^{(S)}(\delta|r) + (1-\eta)\, P_c^{(M)}(\delta). \tag{15}$$

4 Numerical Evaluation

In this section, we numerically evaluate the performance of a typical user at the edge of a building, i.e., $r = R_I$. At this location, the proposed *virtual building approximation* is expected to perform worst.
Spectral efficiency is employed as a metric. It is defined as $\tau = \mathbb{E}_{SIR}[\log_2(1+SIR)]$ and can be reformulated in terms of coverage probability as

$$\tau(r) = \frac{1}{\log(2)} \int_0^{\delta_{max}} \frac{P_c(\delta|r)}{\delta + 1} d\delta, \tag{16}$$

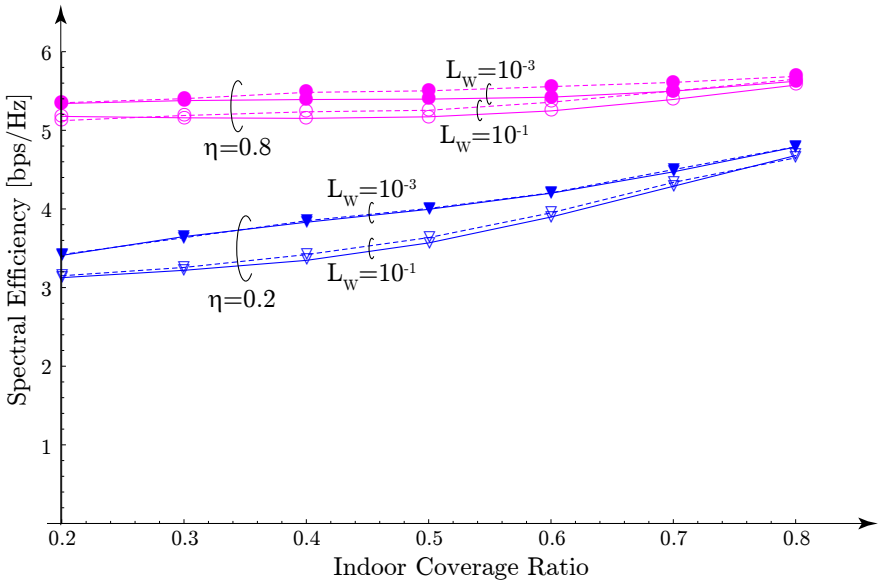

Figure 4: Spectral efficiency [bps/Hz] over area ratio, which is covered by buildings. Solid- and dashed lines denote results from analysis and simulations, respectively. Curves are shown for varying small cell occupation probability (plot markers "$\triangledown$" refer to η = 0.2 and "$\bigcirc$" refer to η = 0.8, respectively) and wall penetration loss, L_{W}.

with $P_{\mathrm{c}}(\delta|r)$ from (15) and $\delta_{\max} = 2^6 - 1$, refering to 64-QAM, which is the highest modulation order in the current Long Term Evolution Advanced (LTE-A) standard [21].
Parameters for evaluation are listed in Table 2. To verify the accuracy of the *virtual building approximation*, Monte Carlo simulations are carried out, using the system model as introduced in sections 2.1 and 2.2. Macro BS density is chosen such that the inscribing ball of the typical cell has R_{c} = 250 m and the BSs are distributed over a field of $15\,R_{\mathrm{c}} \times 15\,R_{\mathrm{c}}$. The results are estimated from averaging over 500 fading- and 500 spatial realizations.
Figure 4 depicts spectral efficiency over indoor coverage ratio, which is defined as $1 - p_{\mathrm{O}}$ in Section 2.2. Note that when fixing the average building *size*, the indoor coverage ratio scales with the *density* of the buildings. Solid- and dashed lines correspond to analysis and simulations, respectively. Results are shown for a sparse- and a dense small cell deployment, as quantified by the occupation probability η. For both scenarios, weak- and strong wall partitioning are investigated. The wall penetration loss is correlated to the building penetration loss γ_{B}, as introduced in (3). In this paper, we conservatively set $\gamma_{\mathrm{B}} = L_{\mathrm{W}}$. This assumption can be replaced by more elaborated models in further work.
It is observed that

- The achievable spectral efficiency is improved by increasing building den-

sity. This result follows the intuition that obstructions due to large objects establish a safeguard against interference [16]. Note that for constant occupation probability, the small cell density grows in proportion to the building density. Therefore, the results render the existence of a *hotspot limited regime* in urban environments questionable and support simulation results in [5, 6, 22, 23].

- Low isolation by wall penetration deteriorates performance in both deployment scenarios. Intuitively, the isolation of the interfering small cells is decreased when the wall penetrations become weaker. The impact of penetration loss on coverage probability, however, becomes minor especially when the building density is high. Intuitively, this indicates that *the number of penetrations rather than the loss per penetration dominates the effect of partitioning between indoor and outdoor environment.*

- Even though we evaluate a user at the edge of a typical building, the analytical results closely resemble the simulations. This confirms the accuracy of the *virtual building approximation* as well as the inclusion of macro interferers in the immediate vicinity of the typical building, as claimed in Section 2.3.

5 Conclusion

In this paper, we introduced a novel system model for two-tier heterogeneous cellular networks in urban environments. We focused on indoor users and derived analytical expressions for the coverage probability in buildings with- and without small cell deployment. Our proposed *virtual building approximation* considerably improved the tractability of the analysis and its accuracy was confirmed by simulation results. Numerically evaluations were carried out to investigate the performance of a *typcial* indoor user in terms of spectral efficiency. The results revealed subtile but crucial effects of an urban environment. Observations such as the blockage safeguard and the vanishing impact of wall isolation with increasing building density have been missed by overly simplistic models. Further work includes physical aspects such as intra-building interference, transmitter-receiver height aspects and a distinction between line-of-sight- and non-line-of-sight dominant interferers.

6 Extensions

The separation between indoor- and outdoor environment revealed crucial effects on the performance of a typical indoor user, which have been overlooked in existing approaches. The results motivate to further refine the physical details.

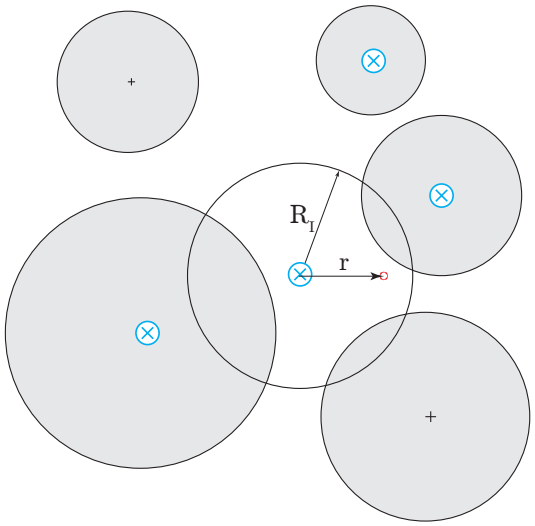

Figure 5: Boolean model for inter-building interference. Central sphere of radius R_{I} corresponds to target building. Spheres of random radius with centers outside a guard of radius R_{I}. Small cells are considered inter-building interferers, if their corresponding sphere overlaps with the target buidling.

The following subsections outline extensions, which are not fully elaborated yet, comprising intra-building interferers, intra-building wall penetration, multistory buildings and Line of Sight (LOS) macro BSs.

6.1 Intra-Building Interference

6.2 Boolean Model

Consider a circularly shaped building of fixed radius R_{I} at the origin. Define a Boolean Model (BM) as a model driven by an independently marked PPP on $\mathbb{R}^d$,

$$\tilde{\Phi} = \sum_i \epsilon_{(x_i, \Xi_i)} \tag{17}$$

with *germs* x_i and *grains*, represented by marks Ξ_i of independent random closed sets on $\mathbb{R}^d$ [18].
The germs of the possibly smallcell occupied indoor areas are located outside the guard region of radius R_G. For simplicity, we assume that $R_G = R_{\mathrm{I}}$, as shown in Figure 5. Each indoor area is occupied by a smallcell with a certain *occupation probability* η. A smallcell is considered an *inter-building small cell*, if the grain of its corresponding indoor area overlaps with the target indoor area. One could imagine a *block of directly bordering houses* in a dense urban environment. The inter-building interferers then comprise an *independently thinned, non homogeneous PPP* Φ_{IB} with *distance dependent intensity*.

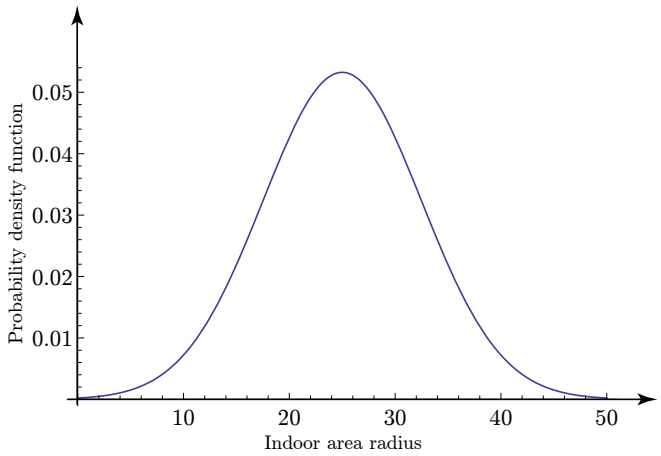

Figure 6: Radius distribution of circular building objects with $\mathbb{E}[R] = 25\,\mathrm{m}$.

6.3 Intensity of Inter-Building Interference Process

Define the point process, which is formed by centers of buildings with radius $(R, R+dR)$ as $\Phi(R)$. $\Phi(R)$ is a subset of the germ point process and constitutes a PPP with density $\lambda_R = \lambda f_R(R)dR$.
Consider the number of centers of circles with radius $(R, R+dR)$ falling into an annular region $\mathcal{A}(0, R', R'+dR')$. Define $A(R') = |\mathcal{A}(0, R', R'+dR')| = 2\pi R' dR'$. Then, the number of centers of circles with radius $(R, R+dR)$ falling into $\mathcal{A}(0, R', R'+dR')$ is Poisson with parameter

$$J(R, R') = \lambda_R A(R') = 2\pi R' dR' \lambda f_R(R) dR \tag{18}$$

In order to intersect with the target building, the minimum radius of the indoor area is $R' - R_\mathrm{I}$. Then, the total number of indoor areas with centers in $\mathcal{A}(0, R', R'+dR')$ and grains intersecting with R_I is Poisson distributed with parameter

$$K(R') = \begin{cases} 2\pi R' dR' \lambda \int_{R'-R_\mathrm{I}}^{\infty} f_R(x)dx & , R' > R_\mathrm{I} \\ 0 & , \text{otherwise} \end{cases} . \tag{19}$$

The results follows intuition that as R_I grows, so does the number of intersecting areas. The building radius distribution $f_R(x)$ has non-negative support and can be chosen such that $\mathbb{E}[R] = R_\mathrm{I}$, as indicated in Figure 6. Then, the intensity of the inhomogeneous PPP is written as $\Lambda(R'dR') = K(R')$.

6.4 Occupied Target Building

Let the target building be occupied by a small cell. Then, the SIR at distance r, $0 < r \leq R_{\mathrm{I}}$ from the origin is calculated as

$$\mathrm{SIR}^{(\mathrm{S})}(r) = \frac{P_{\mathrm{S}} g_0 r^{-\alpha_{\mathrm{I}}}}{\sum_{i:r_i>R_{\mathrm{I}}} P_{\mathrm{S}} g_i L_{\mathrm{W}} r_i^{-\alpha_{\mathrm{I}}} + \sum_{i:R_i>R_{\mathrm{I}}} P_{\mathrm{M}} g_i L_{\mathrm{W}} \ell(R_i)} \tag{20}$$

Note that the signal from the inter-building small cells experience wall penetration L_{W} and log-distance path loss with exponent α_{I}. Due to the asymmetric interference field, the *virtual building*, as introduced in Section 2.4 is applied. Then, along the lines of (40), the coverage probability calculates as

$$\begin{aligned}
P_c^{(\mathrm{S})}(\delta|r) &= \mathbb{P}\left[\mathrm{SIR}^{(\mathrm{S})}(r) > \delta | r\right] \\
&= \mathbb{E}\left[\exp\left(-\frac{\delta r^{\alpha_{\mathrm{I}}}}{P_{\mathrm{S}}} \sum_{i:r_i>R_{\mathrm{I}}} P_{\mathrm{S}} g_i L_{\mathrm{W}} r_i^{-\alpha_{\mathrm{I}}}\right)\right] \\
&\quad \mathbb{E}\left[\exp\left(-\frac{\delta r^{\alpha_{\mathrm{I}}}}{P_{\mathrm{S}}} \sum_{i:R_i>R_{\mathrm{I}}} P_{\mathrm{M}} g_i L_{\mathrm{W}} \ell(R_i)\right)\right] \\
&= \mathbb{E}\left[\prod_{i:r_i>R_{\mathrm{I}}} \exp\left(-\delta r^{\alpha_{\mathrm{I}}} g_i L_{\mathrm{W}} r_i^{-\alpha_{\mathrm{I}}}\right)\right] \\
&\quad \mathbb{E}\left[\prod_{i:R_i>R_{\mathrm{I}}} \exp\left(-\frac{\delta r^{\alpha_{\mathrm{I}}}}{\frac{P_{\mathrm{S}}}{P_{\mathrm{M}}}} g_i L_{\mathrm{W}} \ell(R_i)\right)\right] \\
&= \mathbb{E}_{\Phi_{\mathrm{IB}}}\left[\prod_{i:r_i>R_{\mathrm{I}}} \left(\frac{1}{1+\delta L_{\mathrm{W}}\left(\frac{r}{r_i}\right)^{\alpha_{\mathrm{I}}}}\right)\right] \\
&\quad \mathbb{E}_{\Phi_{\mathrm{M}}}\left[\prod_{i:R_i>R_{\mathrm{I}}} \left(\frac{\frac{P_{\mathrm{S}}}{P_{\mathrm{M}}}}{\frac{P_{\mathrm{S}}}{P_{\mathrm{M}}} + \delta r^{\alpha_{\mathrm{I}}} L_{\mathrm{W}} \ell(R_i)}\right)\right] \\
&\overset{(a)}{=} \exp\left(-2\pi\lambda_{\mathrm{B}} p_{\mathrm{S}} \int_{R_{\mathrm{I}}}^{\infty} \left(\left(1 - \frac{1}{1+\delta L_{\mathrm{W}}\left(\frac{r}{t}\right)^{\alpha_{\mathrm{I}}}}\right) t \int_{t-R_{\mathrm{I}}}^{\infty} f_R(x)dx\right) dt\right), \\
&\quad \exp\left(-2\pi\mu_{\mathrm{M}} \int_{R_{\mathrm{I}}}^{\infty} \left(1 - \frac{\frac{P_{\mathrm{S}}}{P_{\mathrm{M}}}}{\frac{P_{\mathrm{S}}}{P_{\mathrm{M}}} + \delta\, \ell(t) L_{\mathrm{W}} r^{\alpha_{\mathrm{I}}}}\right) t\, dt\right)
\end{aligned} \tag{21}$$

where (a) stems from applying the Probability Generating Functonal (PGFL) with inhomogeneous intensity as defined in Section 6.3. The term $\lambda_{\mathrm{B}}\, p_{\mathrm{S}}$ accounts for the independent thinning of the building process by the small cell occupation probability.

6.5 Non-Occupied Target Building

Inter-Building Small Cell Association. When the target building is not occupied by a small cell, it is assumed that a user associates with the closest inter-building small cell. According to [18, Lemma 3.1.5], the number of overlapping indoor areas with radius distribution $f_R(x)$ is Poisson with parameter

$$\Lambda_{\mathrm{IB}} = 2\pi\lambda_{\mathrm{B}} \int_{R_{\mathrm{I}}}^{\infty} R' \int_{R'-R_{\mathrm{I}}}^{\infty} f_R(x)dxdR'. \tag{22}$$

Then,

$$P_{\mathrm{IB}} = \mathbb{P}\{\text{There are Inter-Building Small Cells}\} = 1 - e^{-p_{\mathrm{S}}\Lambda_{\mathrm{IB}}}, \tag{23}$$

and the distance distribution to the closest small cell is determined as

$$F_{\mathrm{IB},0}(y) = \mathbb{P}[R_{IB,0} < y] = \frac{1 - e^{-2\pi\lambda_{\mathrm{B}}p_{\mathrm{S}}\int_{R_{\mathrm{I}}}^{y} R' \int_{R'-R_{\mathrm{I}}}^{\infty} f_R(x)dxdR'}}{1 - e^{-p_{\mathrm{S}}\Lambda_{\mathrm{IB}}}}. \tag{24}$$

The corresponding density is obtained as

$$f_{\mathrm{IB},0}(y) = \frac{2\pi\lambda_{\mathrm{B}}p_{\mathrm{S}}y\, e^{-2\pi\lambda_{\mathrm{B}}p_{\mathrm{S}}\int_{R_{\mathrm{I}}}^{y} R' \int_{R'-R_{\mathrm{I}}}^{\infty} f_R(x)dxdR'} \int_{y-R_{\mathrm{I}}}^{\infty} f_R(x)dx}{1 - e^{-p_{\mathrm{S}}\Lambda_{\mathrm{IB}}}}. \tag{25}$$

Assume that the user is associated with an inter-building small cell at distance r_0, $r_0 > R_{\mathrm{I}}$. Then, the SIR in a co-tier limited regime calculates as

$$\mathrm{SIR}^{(\mathrm{IB})}(r_0) = \frac{P_{\mathrm{S}}g_0 r_0^{-\alpha_{\mathrm{I}}}}{\sum_{i:R_i>r_0} P_{\mathrm{S}}g_i r_i^{-\alpha_{\mathrm{I}}} + \sum_{i:R_i>R_{\mathrm{I}}} P_{\mathrm{M}}g_i \ell(R_i)}, \tag{26}$$

where L_{W} cancels out since it is experienced by all links.
Along the lines of (21), the conditional coverage probability is found as

$$\begin{aligned} P_c^{(\mathrm{IB})}(\delta|r_0) &= \mathbb{E}_{\Phi_{\mathrm{IB}}}\left[\prod_{i:r_i>r_0}\left(\frac{1}{1+\delta\left(\frac{r_0}{r_i}\right)^{\alpha_{\mathrm{I}}}}\right)\right] \\ &\quad \mathbb{E}_{\Phi_{\mathrm{M}}}\left[\prod_{i:R_i>R_{\mathrm{I}}}\left(\frac{\frac{P_{\mathrm{S}}}{P_{\mathrm{M}}}}{\frac{P_{\mathrm{S}}}{P_{\mathrm{M}}}+\delta r_0^{\alpha_{\mathrm{I}}}\ell(R_i)}\right)\right] \\ &= \exp\left(-2\pi\lambda_{\mathrm{B}}p_{\mathrm{S}}\int_{r_0}^{\infty}\left(\left(1-\frac{1}{1+\delta\left(\frac{r_0}{t}\right)^{\alpha_{\mathrm{I}}}}\right)t\int_{t-R_{\mathrm{I}}}^{\infty} f_R(x)dx\right)dt\right), \\ &\quad \exp\left(-2\pi\mu_{\mathrm{M}}\int_{R_{\mathrm{I}}}^{\infty}\left(1-\frac{\frac{P_{\mathrm{S}}}{P_{\mathrm{M}}}}{\frac{P_{\mathrm{S}}}{P_{\mathrm{M}}}+\delta\,\ell(t)r_0^{\alpha_{\mathrm{I}}}}\right)t\,dt\right) \end{aligned} \tag{27}$$

Table 2: Simulation Parameters

Macro-to-small cell power ratio	$\frac{P_{\mathrm{S}}}{P_{\mathrm{M}}}$	10^{-2}
Macro BS density	μ_{M}	4.61×10^{-6} m^{-2}
Outdoor path loss exponent	α_{O}	4
Indoor path loss exponent	α_{I}	2
Radius of Building Area	R_{I}	25 m

and, by applying (25),

$$P_c^{(\mathrm{IB})}(\delta) = \mathbb{E}_{r_0}\left[P_c^{(\mathrm{IB})}(\delta|r_0)\right] = \int_{R_{\mathrm{I}}}^{\infty} P_c^{(\mathrm{IB})}(\delta|y) f_{\mathrm{IB},0}(y) dy. \tag{28}$$

Dominant Macro BS Association. Consider that the target building is not occupied by a small cell and that there are no inter-building small cells. In this case, the user associates with the dominant macro BS and

$$\mathrm{SIR}^{(\mathrm{M})}(R_0) = \frac{P_{\mathrm{M}} g_0 \ell(R_0)}{\sum_{i:R_i>R_0} P_M g_i \ell(R_i)}. \tag{29}$$

Along the lines of [, Theorem 2], its coverage probability is determined as

$$P_c^{(\mathrm{M})}(\delta) = \mathbb{E}_{R_0}\left[P_c^{(\mathrm{M})}(\delta|R_0)\right] = \int_{R_{\mathrm{I}}}^{\infty} P_c^{(\mathrm{M})}(\delta|R) f_{R_0}(R) dR, \tag{30}$$

where

$$P_{\mathrm{c}}^{(\mathrm{M})}(\delta|R_0) = e^{-2\pi\mu_{\mathrm{M}} I_{\mathrm{M}}}, \tag{31}$$

with

$$I_{\mathrm{M}} = \int_{R_0}^{\infty} \left(1 - \frac{\ell(R_0)}{\ell(R_0) + \delta\, \ell(t)}\right) t\, dt, \tag{32}$$

$$\tag{33}$$

and

$$f_{R_0}(R) = \begin{cases} 2\pi\mu_{\mathrm{M}} R\, e^{-\pi\mu_{\mathrm{M}}(R^2 - R_{\mathrm{I}}^2)} & , \ R \geq R_{\mathrm{I}} \\ 0 & , \ \text{otherwise} \end{cases}. \tag{34}$$

6.6 Numerical Evaluation of Combined Results

Let η denote the small cell occupation probability and P_{IB} be the likelihood that there are inter-building interferers, as given in (23). Then, the coverage

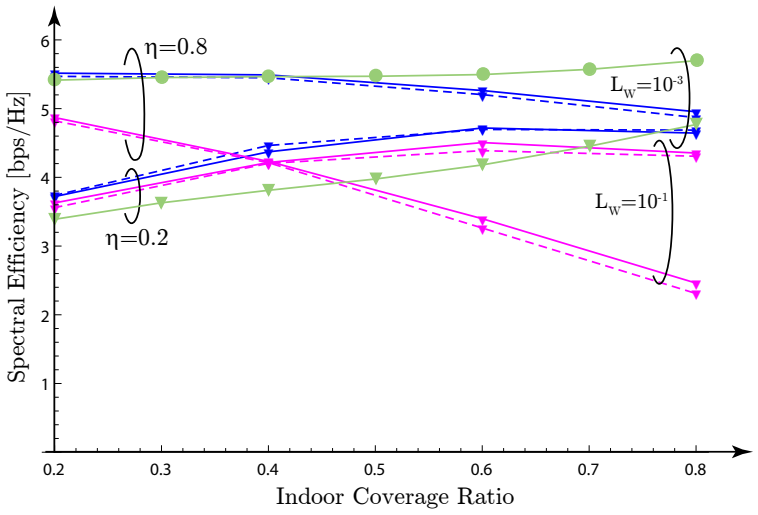

Figure 7: Spectral efficiency [bps/Hz] over indoor area coverage. Blue and magenta curves correspond to $L_{\mathrm{W}} = 10^{-3}$ and $L_{\mathrm{W}} = 10^{-1}$, respectively. Dashed lines show results from Monte Carlos simulations. Green curves correspond to previous results without inter-building small cells and for $L_{\mathrm{W}} = 10^{-3}$.

probability of a *typical* indoor user at distance r from the center of the target building is determined as

$$P_c(\delta) = \eta P_c^{(\mathrm{S})}(\delta|r) + (1-\eta)\left(p_{\mathrm{IB}}\, P_c^{(\mathrm{IB})}(\delta) + (1-p_{\mathrm{IB}}) P_c^{(\mathrm{M})}(\delta)\right). \tag{35}$$

Spectral efficiency is evaluated with the parameters as listed in Table 2. Two different occupation probabilities, $\eta = \{0.2, 0.8\}$, are taken into account. Results are plotted over indoor coverage, as shown in Figure 7.
It is observed that

- At low small cell occupation, $\eta = 0.2$, performance increases with higher indoor coverage. In this case, the interference shielding due to the blockage is exploited. Note that it also outperforms the case without inter-building small cells (green curve), as the likelihood of being associated with an inter-building small cell increases with higher building density. This effect however saturates due to the increasing probability of having more than one small cell within the block of houses and, thus, severe co-tier interference.

- In a sparsely obstructed area (low indoor coverage), performance increases with higher occupation probability. This effect however vanishes in dense urban environments (high indoor coverage) due to the co-tier interference from other inter-building small cells.

- When the wall penetration loss drops from 10^{-3} to 10^{-1}, performance hardly deteriorates in a sparse small cell deployment, $\eta = 0.2$, while it considerably

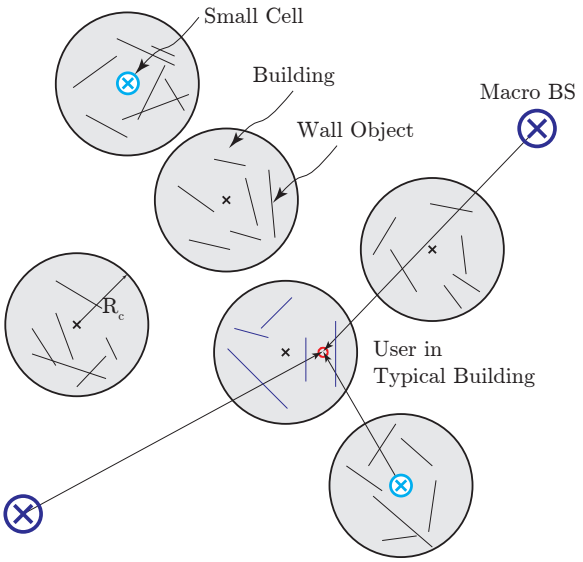

Figure 8: Urban environment with buildings represented by circular objects. Walls within buildings are modeled by a line process.

worsens at $\eta = 0.8$. In both sparse and dense small cell deployments, the sensitivity to wall penetration increases with increasing indoor coverage. This is opposed to previous findings (as shown by green curves) without inter-building interferers and indicates a hot-spot limited regime.

- Results from Monte Carlo simulations show an accurate fit with the analytically obtained curves and verify the applicability of the virtual building approximation.

6.7 Intra-Building Blockage by Walls

Indoor signal propagation is deteriorated by attenuation due to walls, as indicated in Figure 8. Define $w(r)$ as the *relative gain* due to multi-wall loss at distance r. Then, extending (4), the SIR of a smallcell occupied indoor area at distance r, $0 < r < R_{\mathrm{I}}$, formulates as

$$\mathrm{SIR}^{(\mathrm{S})}(r) = \frac{P_{\mathrm{S}} g_0 w(r) r^{-\alpha_{\mathrm{I}}}}{\sum\limits_{i:R_i>R_{\mathrm{I}}} P_{\mathrm{M}} g_i \ell(R_i) + \sum\limits_{i:R_i>2R_{\mathrm{I}}} S_i P_{\mathrm{S}} g_i L_{\mathrm{W}} R_i^{-\alpha_{\mathrm{O}}}}. \tag{36}$$

Then,

$$P_c^{(\mathrm{S})}(\delta|r) = \mathbb{P}\left[\mathrm{SIR}^{(\mathrm{S})}(r) > \delta|r\right] = e^{-2\pi(\mu_{\mathrm{M}} I_{\mathrm{M}} + \mu_{\mathrm{S}} I_{\mathrm{S}})}, \tag{37}$$

where

$$I_{\mathrm{M}} = \int_{R_{\mathrm{I}}}^{\infty} \left(1 - \frac{\frac{P_{\mathrm{S}}}{P_{\mathrm{M}}} w(r)}{\frac{P_{\mathrm{S}}}{P_{\mathrm{M}}} w(r) + \delta\, \ell(t) r^{\alpha_{\mathrm{I}}}} \right) t\, dt \tag{38}$$

$$I_{\mathrm{S}} = \int_{2R_{\mathrm{I}}}^{\infty} \left(\frac{\delta\, L_{\mathrm{W}}\, r^{\alpha_{\mathrm{I}}} e^{-(\beta_{\mathrm{B}} t + p_{\mathrm{B}})}}{w(r) t^{\alpha_{\mathrm{O}}} + \delta\, L_{\mathrm{W}}\, r^{\alpha_{\mathrm{I}}}} \right) t\, dt \tag{39}$$

Proof 3 *Applying (36),*

$$\begin{aligned}
P_c^{(\mathrm{S})}(\delta|r) &= \mathbb{P}\left[\mathrm{SIR}^{(\mathrm{S})}(r) > \delta | r\right] \\
&= \mathbb{E}\left[\exp\left(-\frac{\delta r^{\alpha_{\mathrm{I}}}}{P_{\mathrm{S}} w(r)} \sum_{i:R_i > R_{\mathrm{I}}} P_{\mathrm{M}} g_i \ell(R_i) \right) \right] \\
&\quad \mathbb{E}\left[\exp\left(-\frac{\delta r^{\alpha_{\mathrm{I}}}}{P_{\mathrm{S}} w(r)} \sum_{i:R_i > 2R_{\mathrm{I}}} S_i P_{\mathrm{S}} g_i L_{\mathrm{W}} R_i^{-\alpha_{\mathrm{O}}} \right) \right] \\
&= \mathbb{E}\left[\prod_{i:R_i > R_{\mathrm{I}}} \exp\left(-\frac{\delta r^{\alpha_{\mathrm{I}}}}{\frac{P_{\mathrm{S}}}{P_{\mathrm{M}}} w(r)} g_i \ell(R_i) \right) \right] \\
&\quad \mathbb{E}\left[\prod_{i:R_{\mathrm{I}} > 2R_{\mathrm{I}}} \exp\left(-\frac{\delta r^{\alpha_{\mathrm{I}}}}{w(r)} S_i g_i L_{\mathrm{W}} R_i^{-\alpha_{\mathrm{O}}} \right) \right] \\
&= \mathbb{E}_{\Phi_{\mathrm{M}}}\left[\prod_{i:R_i > R_{\mathrm{I}}} \frac{\frac{P_{\mathrm{S}}}{P_{\mathrm{M}}} w(r)}{\frac{P_{\mathrm{S}}}{P_{\mathrm{M}}} w(r) + \delta\, \ell(R_i) r^{\alpha_{\mathrm{I}}}} \right] \\
&\quad \mathbb{E}_{\Phi_{\mathrm{S}}}\left[\prod_{i:R_i > 2R_{\mathrm{I}}} \left(1 - \frac{\delta\, L_{\mathrm{W}}\, r^{\alpha_{\mathrm{I}}} e^{-(\beta_{\mathrm{B}} R_i + p_{\mathrm{B}})}}{w(r) R_i^{\alpha_{\mathrm{O}}} + \delta\, L_{\mathrm{W}}\, r^{\alpha_{\mathrm{I}}}} \right) \right]
\end{aligned} \tag{40}$$

Note that $\mathrm{SIR}^{(\mathrm{M})}$ and $P_c^{(\mathrm{M})}$ are equivalent to (9) and (33), since the wall loss affects both desired and interfering signals. Similar to the large blockage objects in Section 2.1, wall objects can be modeled by a Boolean scheme. Let $\mathcal{W}$ denote collection of wall objects, represented as lines in $\mathbb{R}^2$:

- The wall centers $w \in \mathcal{W}$, form a PPP of intensity λ_W.
- Attributes of the wall objects, such as length and orientation are mutually independent.
- Sampling, attributes and location of each wall object are independent.

Along the lines of [24], the number of walls crossing a path of length r is Poisson distributed with parameter $\beta_{\mathrm{W}} = 2\lambda_{\mathrm{W}} \mathbb{E}[L]/\pi$, where L is the expected length of a wall. Let $S_{\mathrm{W},i} = \prod_{k=0}^{K_i} \gamma_{\mathrm{W},i,k}$ denote the total power attenuation due to multi-wall loss, where $\gamma_{\mathrm{W},i,k}$ refers to the penetration loss of wall k on link i. Then, assuming

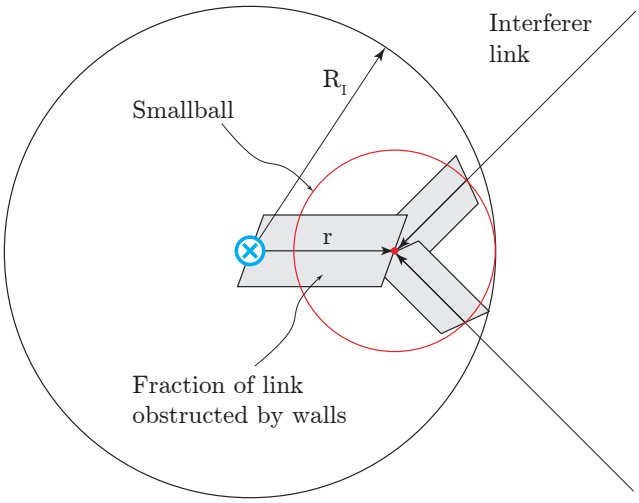

Figure 9: User in small cell occupied building. Smallball approximation is applied for multi-wall propagation loss.

the $\gamma_{\mathrm{W},i,k}$ to be independent and identically distributed (i.i.d.) on $[0,1]$, the n-th moment of $S_{\mathrm{W},i}$ is determined as

$$\mathbb{E}_K[S_{\mathrm{W}}^n] = e^{-\beta_{\mathrm{W}} r(1-\gamma_{\mathrm{W}}^n)}. \tag{41}$$

Note that the model reproduces observations from measurements which state that the single-wall penetration loss decreases with increasing number of traversed walls [25, 26].
Approximate the fraction of the signal path which experiences wall loss by the *smallball* approach [11], as shown in Figure 9. Then $w(r)$ in (36) can be written as

$$w(r) = e^{-\beta_{\mathrm{W}}(2r-R_{\mathrm{I}})(1-\gamma_{\mathrm{W}})} \tag{42}$$

Since $w(r) > 1$ for $2r - R_{\mathrm{I}} < 0$ and $2r - R_{\mathrm{I}} \leq 1$ for $r \geq 0$, the *relative multi-wall penetration loss* appears like a gain at $r < R_{\mathrm{I}}/2$.
Open questions:

- Is the smallball approximation a valid assumption?
- Does the inclusion of the multi-wall loss achieve further insights or is it over-engineered?

6.8 Floor Loss in Multistory Buildings

Similar to wall penetration loss, measurements on intra-building transmission indicate that the loss between floors does not increase linearly with the separation

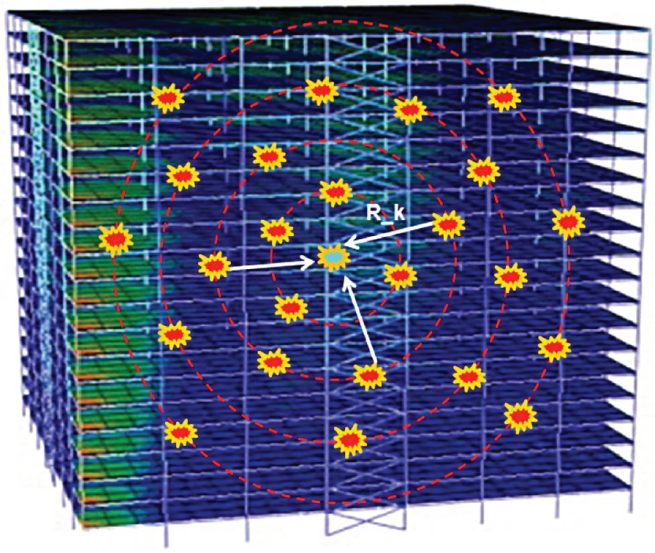

Figure 10: Small cell deployment in a multistory building [28].

distance on a dB scale. In fact, the largest attenuation factor is obtained by separating transmitter and receiver by a single floor [27].
Let S_{F} be a uniformly distributed RV which accounts for the signal attenuation due to a single story. By exploiting

$$\int_0^1 \frac{1}{1+sx} ds = \frac{1}{x} \log(1+x), \tag{43}$$

S_{F} can straightforwardly be incorporated into (20) and (21), respectively.

6.9 LOS Macro BSs

Due to their relevance for conventional homogeneous macro cellular systems, numerous measurement results on outdoor-to-indoor signal propagation are yet available in literature [29–37]. While the campaigns were carried out in considerably different urban environments, the reports commonly agree on the distinct characteristics of LOS- and Non Line of Sight (NLOS) links [30].
For analytical convenience, these characteristics are often condensed into different variances of a log-normally distributed RV, which accounts for the shadowing [32]. While this approximation is valid for far- and medium LOS situations, considerable deviations have been observed in near LOS cases, as present in dense urban environments [30].
The near LOS links can be modeled by free space propagation, while NLOS links experience multi-path propagation and shadowing [30]. We account for these differences by using distinct *path loss exponents* and, in the NLOS case, an additional *shadowing* term.

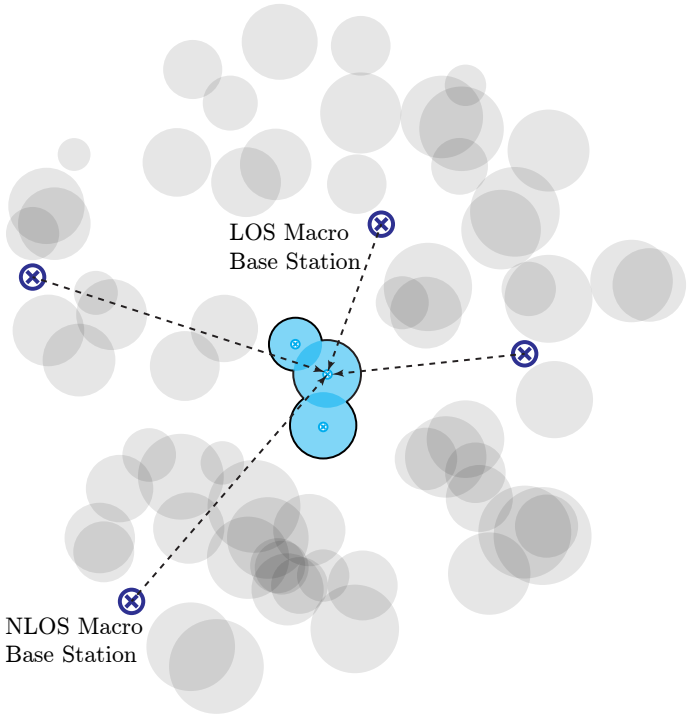

Figure 11: Central target indoor area with intra building interferers from overlapping indoor areas and LOS and NLOS macro BSs. Building density is chosen such that the indoor coverage probability is 50 %.

Interestingly, measurements indicate that the penetration loss of the outer wall is lower in the NLOS case since the multi path components approach the building more frontally [30]. In accordance with the standard [38], we therefore employ distinct *penetration losses* for LOS- and NLOS links. For simplicity, receiver height is omitted in the analysis.
Assume that the shadowing of different links is uncorrelated. Then, the LOS probability of each link is independent and the LOS process Φ_{L} and the NLOS process Φ_{N} form two independent non-homogeneous PPPs. Their density functions are determined as $\mu_{\mathrm{M}}\, v(R)$ and $\mu_{\mathrm{M}}(1-v(R))$, where $v(R) = \exp(-\beta R)$ [39]. An example scenario is shown in Figure 11.
Consider a scenario without co-tier interferers and LOS- as well as NLOS macro BS. Then, the SIR of a user at distance r within a small cell occupied indoor area is calculated as

$$\mathrm{SIR}^{(S)}(r) = \frac{P_{\mathrm{S}} g_0 r^{-\alpha_{\mathrm{I}}}}{\sum_{i:R_i>R_{\mathrm{I}}} P_{\mathrm{M}} L_{\mathrm{L}} g_i R_i^{-\alpha_{\mathrm{L}}} + \sum_{j:R_j>R_{\mathrm{I}}} P_{\mathrm{M}} L_{\mathrm{N}} g_j \ell(R_j)}, \tag{44}$$

where L_{L} and α_{L} denote wall penetration and path loss exponent for the LOS link. The terms $\ell(R_i)$ and L_{N} characterize the NLOS case.

Applying the *virtual building* approximation, the coverage probability at distance r, $0 < r \leq R_{\mathrm{I}}$ is determined as

$$
\begin{aligned}
P_c^{(S)}(\delta|r) &= \mathbb{P}\left[\mathrm{SIR}^{(S)}(r) > \delta|r\right] \\
&= \mathbb{E}_{\Phi_{\mathrm{L}}}\left[\prod_{i:R_i>R_{\mathrm{I}}} \exp\left(-\frac{\delta r^{\alpha_{\mathrm{I}}}}{P_{\mathrm{S}}} P_{\mathrm{M}} L_{\mathrm{L}} g_i R_i^{-\alpha_{\mathrm{L}}}\right)\right] \\
&\quad \mathbb{E}_{\Phi_{\mathrm{N}}}\left[\prod_{j:R_j>R_{\mathrm{I}}} \exp\left(-\frac{\delta r^{\alpha_{\mathrm{I}}}}{P_{\mathrm{S}}} P_{\mathrm{M}} L_{\mathrm{N}} g_j \ell(R_j)\right)\right] \\
&= \mathbb{E}_{\Phi_{\mathrm{L}}}\left[\prod_{i:R_i>R_{\mathrm{I}}} \frac{\frac{P_{\mathrm{S}}}{P_{\mathrm{M}}} R_i^{\alpha_{\mathrm{L}}}}{\frac{P_{\mathrm{S}}}{P_{\mathrm{M}}} R_i^{\alpha_{\mathrm{L}}} + \delta L_{\mathrm{L}} r^{\alpha_{\mathrm{I}}}}\right] \\
&\quad \mathbb{E}_{\Phi_{\mathrm{N}}}\left[\prod_{i:R_j>R_{\mathrm{I}}} \frac{\frac{P_{\mathrm{S}}}{P_{\mathrm{M}}}}{\frac{P_{\mathrm{S}}}{P_{\mathrm{M}}} + \delta\, \ell(R_j) L_{\mathrm{N}} r^{\alpha_{\mathrm{I}}}}\right] \\
&= \exp\left(-2\pi\mu_{\mathrm{M}} \int_{R_{\mathrm{I}}}^{\infty} \left(1 - \frac{\frac{P_{\mathrm{S}}}{P_{\mathrm{M}}} R_i^{\alpha_{\mathrm{L}}}}{\frac{P_{\mathrm{S}}}{P_{\mathrm{M}}} R_i^{\alpha_{\mathrm{L}}} + \delta L_{\mathrm{L}} r^{\alpha_{\mathrm{I}}}}\right) t v(t) dt\right) \\
&\quad \exp\left(-2\pi\mu_{\mathrm{M}} \int_{R_{\mathrm{I}}}^{\infty} \left(1 - \frac{\frac{P_{\mathrm{S}}}{P_{\mathrm{M}}}}{\frac{P_{\mathrm{S}}}{P_{\mathrm{M}}} + \delta\, \ell(R_j) L_{\mathrm{N}} r^{\alpha_{\mathrm{I}}}}\right) t(1 - v(t)) dt\right). \qquad (45)
\end{aligned}
$$

Note that the LOS/NLOS distinction complicates analysis of the *typical indoor user*, since in a *non-occupied* target indoor area it requires to evaluate LOS- and NLOS likelihoods as well as nearest neighbor functions of the non-homogeneous macro BS processes [40].

References

[1] F. Baccelli, B. Blaszczyszyn, and P. Muhlethaler, "Stochastic analysis of spatial and opportunistic aloha," *IEEE Journal on Selected Areas in Communications*, vol. 27, no. 7, pp. 1105–1119, September 2009.

[2] H. Wang and M. Reed, "Tractable Model for Heterogeneous Cellular Networks with Directional Antennas," in *Australian Communications Theory Workshop*, Jan 2012, pp. 61–65.

[3] S. Mukherjee, "UE Coverage in LTE Macro Network with Mixed CSG and Open Access Femto Overlay," in *IEEE International Conference on Communications Workshops (ICC)*, 2011, pp. 1–6.

[4] V. Chandrasekhar, M. Kountouris, and J. Andrews, "Coverage in Tiered Cellular Networks with Spatial Diversity," in *IEEE Global Telecommunications Conference, 2009*, Nov 2009, pp. 1–6.

[5] V. Chandrasekhar, J. Andrews, Z. Shen, T. Muharemovict, and A. Gatherer, "Distributed Power Control in Femtocell-Underlay Cellular Networks," in *IEEE Global Telecommunications Conference, 2009*, Nov 2009, pp. 1–6.

[6] M. K. V. Chandrasekhar and J. G. Andrews, "Coverage in Multi-Antenna Two-Tier Networks," *IEEE Transactions on Wireless Communications*, vol. 8, no. 10, pp. 5314–5327, Dec. 2014.

[7] J. Andrews, F. Baccelli, and R. Ganti, "A Tractable Approach to Coverage and Rate in Cellular Networks," *IEEE Transactions on Communications*, vol. 59, no. 11, pp. 3122–3134, 2011.

[8] V. Chandrasekhar and J. Andrews, "Uplink Capacity and Interference Avoidance for Two-Tier Cellular Networks," in *IEEE Global Telecommunications Conference*, Nov 2007, pp. 3322–3326.

[9] H.-S. Jo, Y. J. Sang, P. Xia, and J. Andrews, "Heterogeneous Cellular Networks with Flexible Cell Association: A Comprehensive Downlink SINR Analysis," *IEEE Transactions on Wireless Communications*, vol. 11, no. 10, pp. 3484–3495, 2012.

[10] S. Mukherjee, "Distribution of downlink sinr in heterogeneous cellular networks," *IEEE Journal on Selected Areas in Communications*, vol. 30, no. 3, pp. 575–585, April 2012.

[11] R. W. Heath, Jr., M. Kountouris, and T. Bai, "Modeling Heterogeneous Network Interference Using Poisson Point Processes," *IEEE Transactions on Signal Processing*, vol. 61, no. 16, pp. 4114–4126, Aug 2013.

[12] V. Chandrasekhar and J. Andrews, "Spectrum Allocation in Tiered Cellular Networks," *IEEE Transactions on Communications*, vol. 57, no. 10, pp. 3059–3068, October 2009.

[13] P. Xia, V. Chandrasekhar, and J. G. Andrews, "Open vs. closed access femtocells in the uplink," *IEEE Transactions on Wireless Communications*, vol. 9, no. 12, pp. 3798–3809, 2010.

[14] H. ElSawy, E. Hossain, and M. Haenggi, "Stochastic Geometry for Modeling, Analysis, and Design of Multi-Tier and Cognitive Cellular Wireless Networks: A Survey," *IEEE Communications Surveys & Tutorials*, vol. 15, no. 3, pp. 996–1019, 2013.

[15] H. Dhillon, R. Ganti, F. Baccelli, and J. Andrews, "Modeling and Analysis of K-Tier Downlink Heterogeneous Cellular Networks," *IEEE Journal on Selected Areas in Communications*, vol. 30, no. 3, pp. 550–560, 2012.

[16] T. Bai, R. Vaze, and R. W. Heath, Jr., "Analysis of Blockage Effects on Urban Cellular Networks," *CoRR*, vol. abs/1309.4141, 2013.

[17] H. ElSawy and E. Hossain, "Two-tier HetNets with Cognitive Femtocells: Downlink Performance Modeling and Analysis in a Multi-Channel Environment," 2013.

[18] F. Baccelli and B. Bllaszczyszyn, *Stochastic Geometry and Wireless Networks: Volume I Theory*, ser. Foundation and Trends in Networking. Now Publishers, March 2009.

[19] G. Boudreau, J. Panicker, N. Guo, R. Chang, N. Wang, and S. Vrzic, "Interference Coordination and Cancellation for 4G networks," *IEEE Communications Magazine*, vol. 47, no. 4, pp. 74–81, April 2009.

[20] M. Haenggi, "On distances in uniformly random networks," *IEEE Transactions on Information Theory*, vol. 51, no. 10, pp. 3584–3586, Oct 2005.

[21] "3GPP TS 36.211 Evolved Universal Terrestrial Radio Access (E-UTRA) physical channels and modulation (release 12)," 3rd Generation Partnership Project (3GPP).

[22] M. Taranetz, J. C. Ikuno, and M. Rupp, "Sensitivity of OFDMA-Based Macrocellular LTE Networks to Femtocell Deployment Density and Isolation," in *International Symposium on Wireless Communication Systems*, Ilmenau, August 2013.

[23] M. Taranetz and M. Rupp, "Performance of Femtocell Access Point Deployments in User Hot-Spot Scenarios," in *Australasian Telecommunication Networks and Applications Conference*, Brisbane, Australia, November 2012.

[24] T. Bai, R. Vaze, and R. W. Heath, Jr., "Using Random Shape Theory to Model Blockage in Random Cellular Networks," in *International Conference on Signal Processing and Communications (SPCOM)*, July 2012, pp. 1–5.

[25] M. Lott and I. Forkel, "A Multi-Wall-and-Floor Model for Indoor Radio Propagation," in *IEEE VTS 53rd Vehicular Technology Conference*, vol. 1, 2001, pp. 464–468 vol.1.

[26] P. Karlsson, C. Bergljung, E. Thomsen, and H. Borjeson, "Wideband measurement and analysis of penetration loss in the 5 ghz band," in *Vehicular Technology Conference, 1999. VTC 1999 - Fall. IEEE VTS 50th*, vol. 4, 1999, pp. 2323–2328 vol.4.

[27] J. Andersen, T. Rappaport, and S. Yoshida, "Propagation measurements and models for wireless communications channels," *Communications Magazine, IEEE*, vol. 33, no. 1, pp. 42–49, Jan 1995.

[28] "High-Capacity Indoor Wireless Solutions: Picocell or Femtocell?" Fujitsu Network Communications Inc., Tech. Rep., March 2013.

[29] P. J. Barry and A. Wiliamson, "Statistical model for uhf radio-wave signals within externally illuminated multistorey buildings," *Communications, Speech and Vision, IEE Proceedings I*, vol. 138, no. 4, pp. 307–318, Aug 1991.

[30] R. Gahleitner and E. Bonek, "Radio Wave Penetration into Urban Buildings in Small Cells and Microcells," in *IEEE 44th Vehicular Technology Conference*, Jun 1994, pp. 887–891 vol.2.

[31] Y. Corre, J. Stephan, and Y. Lostanlen, "Indoor-to-Outdoor Path-Loss Models for Femtocell Predictions," in *IEEE 22nd International Symposium on Personal Indoor and Mobile Radio Communications (PIMRC)*, Sept 2011, pp. 824–828.

[32] A. De Toledo and A. M. d. Turkmani, "Propagation into and within buildings at 900, 1800 and 2300 mhz," in *Vehicular Technology Conference, 1992, IEEE 42nd*, May 1992, pp. 633–636 vol.2.

[33] C. Oestges, N. Czink, B. Bandemer, P. Castiglione, F. Kaltenberger, and A. Paulraj, "Experimental Characterization and Modeling of Outdoor-to-Indoor and Indoor-to-Indoor Distributed Channels," *IEEE Transactions on Vehicular Technology*, vol. 59, no. 5, pp. 2253–2265, Jun 2010.

[34] D. M. J. Devasirvatham, C. Banerjee, M. Krain, and D. A. Rappaport, "Multi-Frequency Radiowave Propagation Measurements in the Portable Radio Environment, year=1990, month=Apr, pages=1334-1340

vol.4, doi=10.1109/ICC.1990.117286,," in *IEEE International Conference on Communications*.

[35] A. Valcarce and J. Zhang, "Empirical Indoor-to-Outdoor Propagation Model for Residential Areas at 0.9 and 3.5 GHz," *IEEE Antennas and Wireless Propagation Letters*, vol. 9, pp. 682–685, 2010.

[36] A. De Toledo, A. M. d. Turkmani, and J. Parsons, "Estimating coverage of radio transmission into and within buildings at 900, 1800, and 2300 mhz," *IEEE Personal Communications*, vol. 5, no. 2, pp. 40–47, Apr 1998.

[37] A. Turkmani and A. De Toledo, "Modelling of radio transmissions into and within multistorey buildings at 900,1800 and 2300 mhz," *IEEE Proceedings on Communications, Speech and Vision*, vol. 140, pp. 462–470(8), December 1993.

[38] 3rd Generation Partnership Project, "TR 36.814: Evolved Universal Terrestrial Radio Access (E-UTRA); Further advancements for E-UTRA physical layer aspects," 3rd Generation Partnership Project, Tech. Rep., March 2010.

[39] T. Bai and R. Heath, "Coverage analysis for millimeter wave cellular networks with blockage effects," in *IEEE Global Conference on Signal and Information Processing (GlobalSIP)*, Dec 2013, pp. 727–730.

[40] T. Bai and R. W. H. Jr., "Coverage and Rate Analysis for Millimeter Wave Cellular Networks," *CoRR*, vol. abs/1402.6430, 2014.